Journal of Alloys and Compounds, 194 (1993) 31–40
JALCOM 524

Hydrogenation and nitrogenation of $SmFe_2$

Chris N. Christodoulou and Takuo Takeshita
Central Research Institute, Mitsubishi Materials Corporation, 1-297 Kitabukuro-cho, Omiya, Saitama 330 (Japan)

(Received September 7, 1992)

Abstract

The characteristics of the reactions between $SmFe_2$ and H_2 or N_2 were studied by isochorothermal analysis, X-ray diffraction and thermomagnetic analysis. Under hydrogen pressures of below 150 kPa, $SmFe_2$ absorbs hydrogen instantaneously and exothermically at temperatures of between 120 and 160 °C. When hydrogenation occurs in an "excess of hydrogen gas", the reaction products are dependent on the maximum hydrogenation temperature: unreacted $SmFe_2$, $SmFe_2$ hydride, amorphous (Sm,Fe_2) hydride, Sm hydride and α-Fe. When hydrogenation occurs in a "deficient hydrogen gas" atmosphere, Sm_2Fe_{17}, $SmFe_3$ and Sm are also found in the reaction products, depending on the maximum hydrogenation temperature. The amorphous ($SmFe_2$) hydride begins to decompose into an Sm-poorer amorphous (Sm,Fe_2) hydride and Sm hydride immediately after its formation. At about 325 °C, α-Fe also begins to crystallize and the composition of the amorphous phase varies continuously. The Curie temperatures of $SmFe_2$, $SmFe_2$ hydride and amorphous (Sm,Fe_2) hydride are 683 K, 110 K and 348–508 K (depending on the metal composition and hydrogen content) respectively. On heating under vacuum, the amorphous (Sm,Fe_2) hydride begins to lose hydrogen at temperatures of between 160 and 200 °C with simultaneous decomposition into Sm hydride and an Sm-poorer amorphous phase. The reaction of $SmFe_2$ powder with N_2 begins at about 250 °C with the formation of SmN, α-Fe and Sm. At high temperatures (950 °C), only SmN and α-Fe exist. When bulk $SmFe_2$ is used instead of powder, the reaction is not complete (even at 950 °C) and $SmFe_3$ begins to appear. No interstitial $SmFe_2$ nitride was formed at any temperature.

1. Introduction

The RT_2 (where R ≡ rare earth, T ≡ Fe, Co or Ni) intermetallic compounds possess the cubic Laves-phase $MgCu_2$ type crystal structure. They absorb appreciable amounts of hydrogen [1–3] resulting in either crystalline or amorphous RT_2 hydrides (hydrogen-induced amorphization or HIA). Of the RFe_2 compounds (R ≡ Ce, Sm, Gd, Td, Dy, Ho, Er and Y) [1], only Ce does not form crystalline hydride; it directly forms amorphous hydride [4, 5]. Many aspects of the reaction between $SmFe_2$ intermetallic compound and hydrogen have been studied by Kost *et al.* [6], Aoki *et al.* [7] and Jones *et al.* [8]. No nitrogenation study on $SmFe_2$ has been reported in the literature.

The discovery of a new magnetic material, Sm_2Fe_{17} nitride [9], has triggered a renewed interest in the Sm–Fe intermetallic compounds in general. Permanent magnets have already been prepared based on the Sm_2Fe_{17} nitride by several methods such as mechanical alloying (MA) [10, 11], rapid solidification [12, 13], conventional powder metallurgy [11, 14, 15] and hydrogen treatment (HDDR) [16, 17]. All of these methods involve two major steps: (a) the formation of the Sm_2Fe_{17} phase (preferably in a microcrystalline form) and (b) the nitrogenation of Sm_2Fe_{17} in N_2 or ammonia to form the (interstitial) Sm_2Fe_{17} nitride which exhibits hard magnetic properties.

Many studies have been published on the Sm_2Fe_{17} nitrides, mainly concerning the nitrogenation kinetics [18, 19] and substitutions [9, 20–25] of Sm or Fe with other rare earth or transition metals respectively. In step (a) of the preparation method, one usually has to deal not only with the major Sm_2Fe_{17} phase but also with other phases such as Sm, $SmFe_2$, $SmFe_3$ and α-Fe. Consequently, during the whole process (steps (a) and (b)), one has to consider the reactions of these "secondary" phases with hydrogen and nitrogen. The reaction products have an effect on the details of the processes as well as on the magnetic properties of the final product. The experiences with other magnetic materials, such as the $Nd_2Fe_{14}B$-based magnets, show that the presence of secondary phases plays an important role in the development of the intrinsic coercivity. At present, there is no adequate specific information on the characteristics of the reactions between the Sm–Fe alloys and hydrogen or nitrogen.

The lack of such information has led us to make a series of studies on the reactions between Sm [26], $SmFe_2$, $SmFe_3$ and Sm_2Fe_{17} and hydrogen or nitrogen

0925-8388/93/$6.00

gas as a function of temperature and gas pressure. In the present paper, the reactions between $SmFe_2$ and H_2 or N_2 are reported. The reactions of H_2 and N_2 with the other phases ($SmFe_3$ and Sm_2Fe_{17}) will be reported in the near future. Such information on the reactions between the Sm–Fe alloys and H_2 or N_2 has been used to interpret the resulting phases and magnetic properties of the Sm_2Fe_{17} nitride-based permanent magnets prepared in our laboratory by several methods. These will also be published in the near future.

In the presentation of the results, a letter "a" is added to the front of the chemical formula of the amorphous phase in order to distinguish it from the crystalline phases.

2. Experimental details

The $SmFe_2$ alloy was prepared by arc melting of the constituent elements (purity, better than 99.9 wt.%) in a pure argon gas atmosphere. During melting, 5 wt.% Sm excess was added to account for the Sm loss due to vaporization. The as-prepared $SmFe_2$ alloy was heat treated at 600 °C for about 1 week in order to produce an $SmFe_2$ single-phase alloy. The purity of H_2 and N_2 gases used for hydrogenation and nitrogenation was higher than 99.999 vol.%.

The constant volume reactor (isochorothermal analyser or ITA) which was used in the present study is similar to the thermopiezic analyser (TPA) used by other researchers (for instance, Coey *et al.* [9]) for the study of gas–solid reactions. The volume of the ITA was about 2.3 cm^3 and only about 5% of the total volume was heated. The $SmFe_2$ samples, weighing between 2 and 12 mg, were placed in a quartz tube (ITA) and heated with a precisely controlled programmable furnace capable of reaching a temperature of 1000 °C. The pressure was measured with a pressure sensor capable of detecting pressure differences of about 100 Pa. The temperature was measured with an accuracy of ± 1 °C. The pressure *vs.* temperature data were collected in a computer and analysed by taking into consideration the pressure variations due to the thermal effects (heated volume). By utilizing the ideal gas law, the data were transformed and plotted in terms of gas atoms absorbed by or desorbed from one mole of solid as a function of temperature. The ideal gas law which was applied in the case of hydrogen and nitrogen is considered to be a very good approximation since the pressure–temperature conditions (0–150 kPa and 20–1000 °C) are far above their corresponding critical values. ITA isochores were obtained for the "$SmFe_2 + H_2$" and "$SmFe_2 + N_2$" systems in the temperature range 20–950 °C.

Phase analysis was performed by thermomagnetic analysis (TMA) and powder X-ray diffraction (XRD). Thermomagnetic measurements were performed with a vibrating sample magnetometer (VSM) for temperatures below 25 °C and a Faraday balance for temperatures of between 25 and 900 °C in a magnetic field up to 15 kOe. The samples used in the Faraday balance were sealed in a quartz tube of known volume under argon or hydrogen gas depending on the scope of the experiment. XRD patterns were obtained under ambient conditions using a Philips automated diffractometer with Cu Kα radiation monochromated with a graphite single crystal. XRD patterns were obtained for both random powder and magnetically aligned powder which was fixed in epoxy resin.

3. Results and discussion

3.1. Crystal structure and magnetic properties of $SmFe_2$

The XRD pattern of the $SmFe_2$ alloy used in the present study is shown in Fig. 1. The alloy contains only the $SmFe_2$ phase which crystallizes in the f.c.c. $MgCu_2$-type structure (Laves phase) with a lattice parameter a of 7.404 Å. The absence of the $SmFe_3$ phase was confirmed by the XRD pattern of the aligned powder (Fig. 1(b)) which does not show any c-axis Bragg peaks (*i.e.* (006), (009) or (00$\underline{12}$)); these should be observed even if a small amount of the magnetically uniaxial $SmFe_3$ phase is present. In the same pattern, there is a relative increase in the intensities of the (111) and (222) Bragg peaks corresponding to the $SmFe_2$

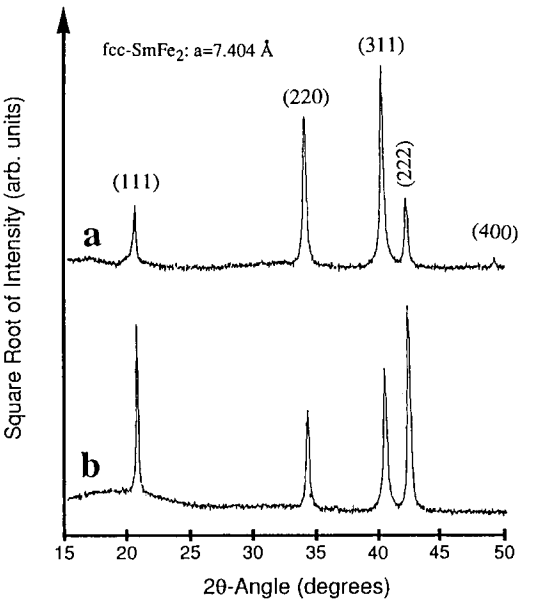

Fig. 1. XRD patterns of the $SmFe_2$ alloy: (a) Random powder; (b) aligned powder in a magnetic field of 20 kOe at room temperature.

phase. This is expected because the easy direction of magnetization (EDOM) at room temperature is along the ⟨111⟩ crystallographic direction [27]. The Curie temperature (T_c) of the $SmFe_2$ phase is 410 °C as shown in the TMA trace in Fig. 2. The TMA trace in Fig. 2 provides additional evidence that the alloy does not contain any other ferromagnetic phase (Sm_2Fe_{17} with $T_c = 135$ °C, $SmFe_3$ with $T_c = 390$ °C and α-Fe with $T_c = 770$ °C), except $SmFe_2$ ($T_c = 410$ °C). The saturation magnetization (M_s) of the $SmFe_2$ phase was measured with the VSM to be 51.2 e.m.u g^{-1} at the maximum available field of 15 kOe.

3.2. *Reaction of $SmFe_2$ with hydrogen*

Hydrogenation of the $SmFe_2$ phase was performed under "deficient hydrogen gas" and "excess hydrogen gas" atmospheres. The term "deficient hydrogen gas" atmosphere means that the initial ratio of hydrogen gas atoms per mole of $SmFe_2$ is lower than 3.35, a value which will be shown later to represent the maximum amount of hydrogen that one mole of $SmFe_2$ can absorb under any conditions used in the present study. The term "excess hydrogen gas" atmosphere means that the initial ratio of hydrogen gas atoms per mole of $SmFe_2$ is much greater than 3.35. Both experiments provide useful information on the initial stage of hydrogen absorption and the progress of the hydrogenation reaction in terms of the intermediate and final reaction products at different hydrogenation temperatures.

3.2.1. *Hydrogenation*

3.2.1.1. Isochorothermal analysis. Figure 3 shows the ITA trace for the "$SmFe_2 + H_2$" system with an initial ratio of 1.33 H gas atoms per mole of $SmFe_2$ (at room temperature). The reaction is initiated at 136 °C with the absorption of 1.18 H atoms per mole of $SmFe_2$.

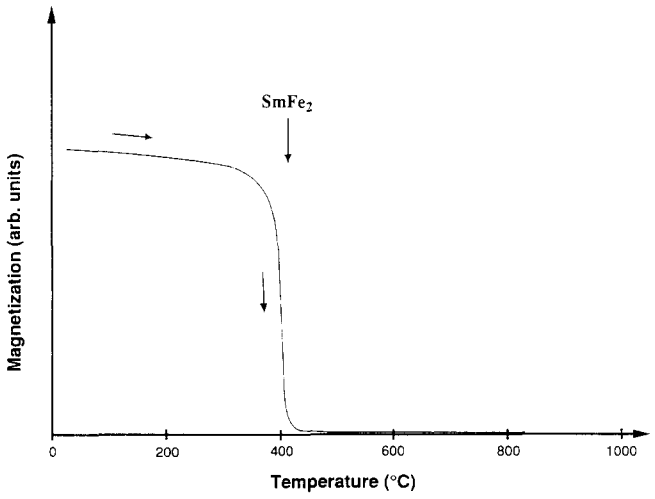

Fig. 2. TMA trace of the $SmFe_2$ alloy.

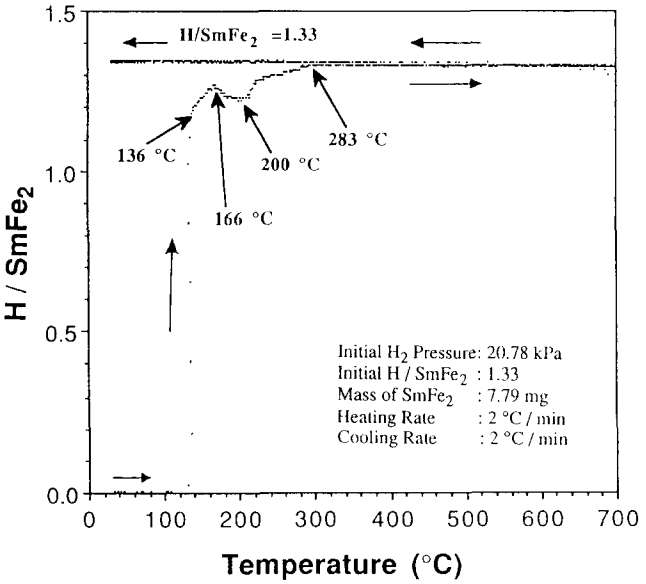

Fig. 3. ITA trace for the "$SmFe_2 + H_2$" system under an initial ratio of $H/SmFe_2 = 1.33$ (under a "deficient hydrogen gas" atmosphere).

The products of the initial hydrogen absorption are unreacted $SmFe_2$, $SmFe_2$ hydride, a-(Sm,Fe_2) hydride and Sm hydride. $SmFe_2$ continues to absorb hydrogen slowly reaching a peak value of 1.27 at 166 °C. Subsequently, it begins to desorb hydrogen gradually reaching a value of 1.22 H atoms per mole of $SmFe_2$ at 200 °C. This desorption process is mainly due to the interstitial desorption of hydrogen from the $SmFe_2$ hydride which reforms some of the $SmFe_2$. Finally, the hydrogen concentration increases monotonically reaching the maximum attainable value of 1.33 at 283 °C and remains constant up to the maximum temperature of 700 °C and also during cooling. Above a temperature of 283 °C, the entire amount of hydrogen is contained originally in the form of a mixture of a-(Sm,Fe_2) hydride + Sm hydride and then exclusively (in the higher temperature range) in the form of Sm hydride.

Figure 4 shows the ITA trace for the "$SmFe_2 + H_2$" system with an initial ratio of 25.04 H gas atoms per mole of $SmFe_2$ (at room temperature). This particular ITA trace was obtained by raising the temperature up to a certain value (175, 250, 450 and 700 °C) followed by cooling to temperatures below 100 °C. Hydrogen absorption occurs instantly at 145 °C with 1 mol of $SmFe_2$ absorbing 3.12 hydrogen atoms. Subsequent cooling to room temperature causes a further hydrogen absorption (3.35 H atoms per $SmFe_2$). As the temperature increases, the hydrogen concentration decreases. The successive heating and cooling causes an irreversible decrease in the hydrogen concentration which is most evident after cooling to temperatures below 100 °C. This is due to the continuous precipitation of Sm hydride which, in general, can "carry" less

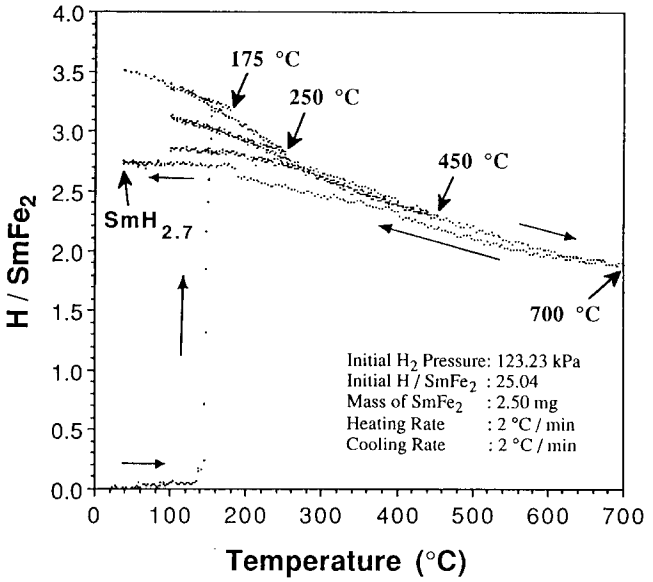

Fig. 4. ITA trace for the "$SmFe_2+H_2$" system under an initial ratio of $H/SmFe_2=25.04$ (under an "excess hydrogen gas" atmosphere).

hydrogen than the a-(Sm,Fe_2) hydride at the same temperature [26]. On cooling from a temperature of 700 °C, only α-Fe and Sm hydride are formed. The cooling part of the ITA trace in Fig. 4 exhibits common features with the "$Sm+H_2$" system [26] which was studied in our laboratory. The further absorption of hydrogen at about 190 °C (during cooling) and the resulting final composition of $SmH_{2.7}$ are two common features. In Fig. 3, these features are not present because of the unavailability of hydrogen.

3.2.1.2. X-ray diffraction. Samples of $SmFe_2$ were hydrogenated inside the ITA under the same conditions used for the ITA trace shown in Fig. 3, and were heated up to 160 (a), 200 (b), 300 (c), 450 (d) and 700 °C (e) followed by cooling to room temperature. The corresponding XRD patterns are shown in Figs. 5(a)–5(e). Sample (a) contains more unreacted $SmFe_2$ and $SmFe_2$ hydride and less Sm hydride and a-(Sm,Fe_2) hydride than sample (b). The existence of the amorphous phase is suggested by the absence of the α-Fe Bragg peaks (since some of the $SmFe_2$ decomposes into Sm hydride) and by the TMA experiments which are presented later. In addition, the existence of a-(Sm,Fe_2) hydride is also confirmed by transmission electron microscopy (TEM) studies reported by Aoki *et al.* [7]. The lattice parameters of the f.c.c. $SmFe_2$ hydride varies from $a=7.66$ Å to $a=7.77$ Å. This corresponds to a maximum lattice expansion of about 16%. In sample (c), the amount of unreacted $SmFe_2$ is decreased and the amounts of a-(Sm,Fe_2) hydride (broad Bragg peaks) and Sm hydride are increased. No $SmFe_2$ hydride is present in this sample. Up to the hydrogenation temperature of 300 °C, all of the Fe formed due to the decomposition of $SmFe_2$ is contained within the amorphous phase. Sample (d) contains approximately the same amount of unreacted $SmFe_2$ as sample (c) but more Sm hydride. Also, the a-(Sm,Fe_2) hydride phase has disappeared and the crystalline α-Fe appears instead. In addition, some poorly crystallized Sm appears simultaneously with α-Fe. The presence of Sm is supported by the appearance of the f.c.c. SmO [26] in the XRD pattern of Fig. 5(d). The crystallization of the a-(Sm,Fe_2) hydride causes the initial formation of Sm

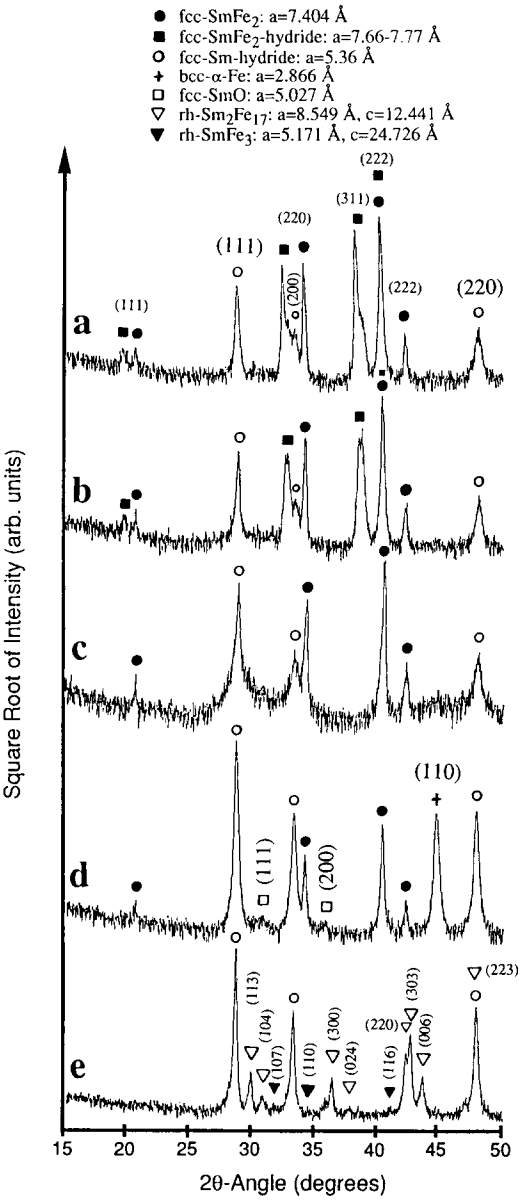

Fig. 5. XRD patterns of $SmFe_2$ samples hydrogenated under an initial ratio of $H/SmFe_2=1.33$ (under a "deficient hydrogen gas" atmosphere) at temperatures of (a) 160 °C, (b) 200 °C, (c) 300 °C, (d) 450 °C and (e) 700 °C. Samples (a), (b) and (c) also contain a-(Sm,Fe_2) hydride.

hydride and, therefore, the remaining amorphous phase enriched in Fe crystallizes with the precipitation of a metastable mixture of α-Fe and Sm. Sample (e) which was hydrogenated at a temperature of 700 °C contains Sm hydride, Sm_2Fe_{17} and $SmFe_3$. No $SmFe_2$, α-Fe or Sm are found in this sample. At a temperature of 700 °C, the metastable mixture of α-Fe + Sm, together with the unreacted $SmFe_2$, react to form Sm_2Fe_{17} and $SmFe_3$ which are the equilibrium phases. This is due to the fact that hydrogen ties up a portion of Sm (in the form of stable Sm hydride) and the overall binary metal composition is shifted to the compositions between Sm_2Fe_{17} and $SmFe_3$. Therefore, under equilibrium conditions we expect to detect only these two phases.

Samples of $SmFe_2$ were also hydrogenated in the ITA under the same conditions used for the ITA experiment shown in Fig. 4 with heating up to 145 (a), 150 (b), 200 (c), 300 (d), 425 (e) and 700 °C (f) followed by cooling to room temperature. The XRD patterns are shown in Figs. 6(a)–6(f). These show that samples (a) and (b) consist of a decreasing amount of unreacted $SmFe_2$ and increasing amounts of $SmFe_2$ hydride, a-(Sm,Fe_2) hydride (suggested by the broad Bragg peaks) and Sm hydride. The lattice parameter of the f.c.c. $SmFe_2$ hydride varies from $a = 7.67$ Å to $a = 8.08$ Å. This corresponds to a maximum lattice expansion of about 30%. Samples (c), (d) and (e) contain a decreasing amount of a-(Sm,Fe) hydride and an increasing amount of Sm hydride. No $SmFe_2$ or $SmFe_2$ hydride are found in these samples. The appearance of α-Fe at a temperature of 425 °C (Fig. 6(e)) or above (Fig. 6(f)) is a result of the decomposition of the a-(Sm,Fe_2) hydride in the presence of hydrogen gas into α-Fe + Sm hydride. It is worth noting that up to the hydrogenation temperature of 300 °C, Fe is contained entirely in the amorphous phase (Fig. 6(d)) contrary to Sm which is crystallized partially forming Sm hydride. Also, the end products (after hydrogenation at 700 °C) are only α-Fe and Sm hydride. This is different from hydrogenation under a "deficient hydrogen gas" atmosphere which was described above. This is because, during the crystallization of the amorphous phase, hydrogen is readily available to react with the entire amount of Sm, forming stable Sm hydride, and therefore the elemental α-Fe remains unaffected even at high temperatures.

3.2.1.3. Thermomagnetic analysis. Figure 7 shows the TMA trace of sample (a) in Fig. 5. Before obtaining the TMA trace, the sample was sealed in a small quartz tube under an argon gas atmosphere. Previously, this sample was shown (Fig. 5(a)) to consist of a mixture of unreacted $SmFe_2$, $SmFe_2$ hydride, a-(Sm,Fe_2) hydride and Sm hydride. The Curie temperatures (T_c) of $SmFe_2$ hydride, a-(Sm,Fe_2) hydride and $SmFe_2$ are 110 K, 235 °C and 410 °C respectively. These results are very

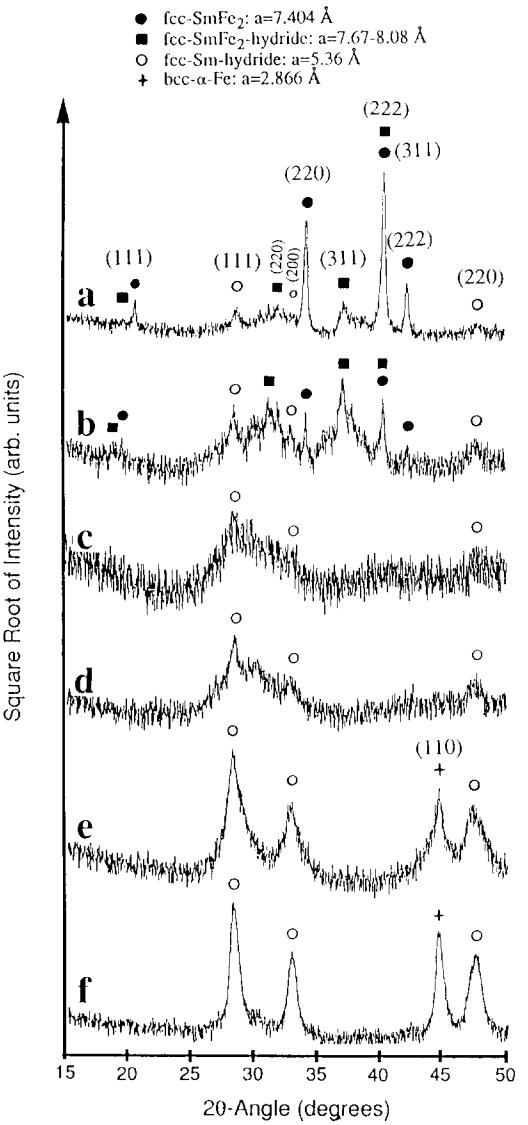

Fig. 6. XRD patterns of $SmFe_2$ samples hydrogenated under an initial ratio of $H/SmFe_2 = 25.04$ (under an "excess hydrogen gas" atmosphere) at temperatures of (a) 145 °C, (b) 150 °C, (c) 200 °C, (d) 300 °C, (e) 425 °C and (f) 700 °C. Samples (a), (b), (c) and (d) also contain a-(Sm,Fe_2) hydride. Sample (e) contains a-(Sm,Fe) hydride.

similar to those obtained by Aoki *et al.* [28] for the $GdFe_2$ intermetallic compound.

Figure 8 shows the TMA trace of an $SmFe_2$ sample sealed in a quartz tube under hydrogen gas with an initial ratio of H atoms to $SmFe_2$ moles of about 1.4 (at room temperature). On heating, there is an irreversible change in the magnetization which is due to the absorption of hydrogen forming a mixture of interstitial $SmFe_2$ hydride ($T_c \approx 110$ K and therefore its magnetization is lost), a-(Sm,Fe_2) hydride and Sm hydride (Figs. 5(a) and 5(b)). Almost immediately after hydrogen absorption, the magnetization begins to increase because the $SmFe_2$ hydride begins to desorb hydrogen reforming $SmFe_2$ ($T_c = 410$ °C). Subsequently,

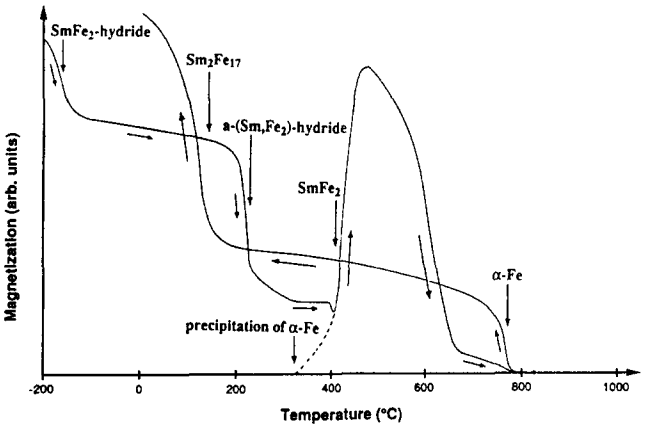

Fig. 7. TMA trace of an $SmFe_2$ sample hydrogenated under H/$SmFe_2$=1.33 at a temperature of 160 °C and sealed under an argon gas atmosphere. It contains $SmFe_2$, $SmFe_2$ hydride, a-(Sm,Fe_2) hydride and Sm hydride. The hypothetical broken line shows the temperature (325 °C) where precipitation of α-Fe occurs.

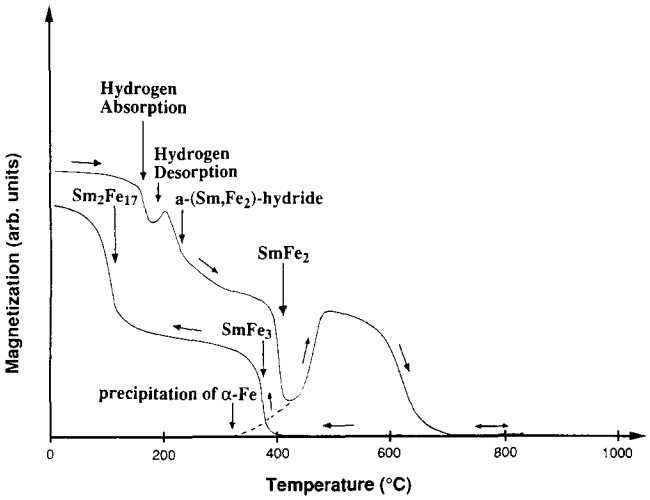

Fig. 8. TMA trace of an $SmFe_2$ sample sealed under a "deficient hydrogen gas" atmosphere with an initial ratio of H/$SmFe_2$=1.4. The hypothetical broken line shows the temperature (325 °C) where the precipitation of α-Fe occurs.

the magnetization decreases due to the fact that the released hydrogen reacts again with a portion of $SmFe_2$. The Curie temperature at 410 °C reveals the presence of unreacted $SmFe_2$. The sharp increase in the magnetization at about 410 °C is due to the precipitation of α-Fe during the crystallization of the a-(Sm,Fe_2) hydride; this is actually initiated at lower temperatures (approximately 325 °C) as shown by the fact that the magnetization does not disappear at 410 °C. At a temperature of 475 °C all hydrogen is tied up with a portion of Sm in the form of Sm hydride and the overall composition of the remaining metals falls between the compositions of Sm_2Fe_{17} and $SmFe_3$. Therefore, at relatively high temperatures, the equilibrium phases Sm_2Fe_{17} (T_c=135 °C) and $SmFe_3$ (T_c=390 °C) appear as shown in the TMA trace on cooling from 840 °C.

Figure 9 shows the TMA trace of an $SmFe_2$ sample hydrogenated at 300 °C and sealed inside a quartz tube under an argon gas atmosphere. Previously, this sample was shown (Fig. 6(d)) to consist of a mixture of a-(Sm,Fe_2) hydride and Sm hydride. The Curie temperature of the a-(Sm,Fe_2) hydride is about 150 °C. The increase in the magnetization at about 325 °C is attributed to the crystallization of the amorphous phase into α-Fe+Sm hydride. The Curie temperature of α-Fe is 770 °C and therefore, at a temperature of 325 °C, the precipitating α-Fe causes an increase in the magnetization of the sample. As the temperature increases, more α-Fe and Sm hydride precipitate. The precipitation of α-Fe seems to be terminated at a temperature of about 450 °C. Above this temperature only α-Fe and Sm hydride exist. This is evident from the cooling part of the TMA trace (Fig. 9) where only the T_c of α-Fe is present. All of the Sm is tied up with hydrogen in the form of Sm hydride and therefore there is no Sm available to recombine with α-Fe at high temperatures and form other phases. This was also seen previously in the XRD pattern shown in Fig. 5(f).

Figure 10 shows the TMA trace of an $SmFe_2$ sample which was sealed in a quartz tube under hydrogen gas with an initial ratio of 4.8 H atoms per mole of $SmFe_2$ (at room temperature). This is similar to the TMA trace in Fig. 8 except that, after interstitial hydrogen desorption, the readily available hydrogen gas reacts with the entire amount of unreacted $SmFe_2$ forming a-(Sm,Fe_2) hydride and Sm hydride. This is why the magnetization of the sample goes through zero. At about 325 °C, α-Fe begins to crystallize from the amor-

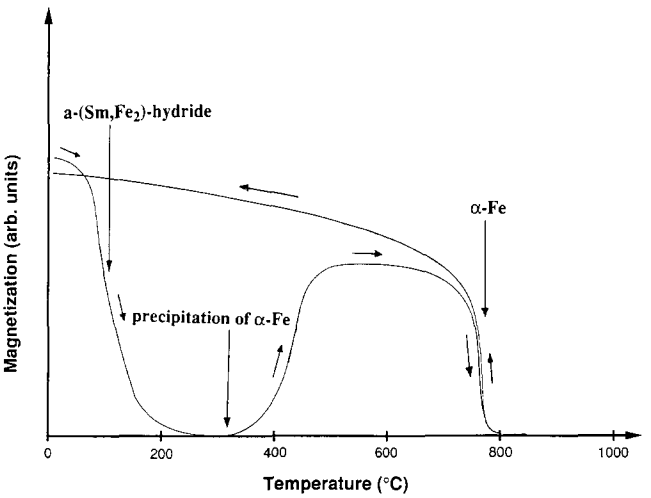

Fig. 9. TMA trace of an $SmFe_2$ sample hydrogenated under an initial ratio of H/$SmFe_2$=25 at a temperature of 300 °C and sealed under an argon gas atmosphere. It contains a-(Sm,Fe_2) hydride and a little Sm hydride.

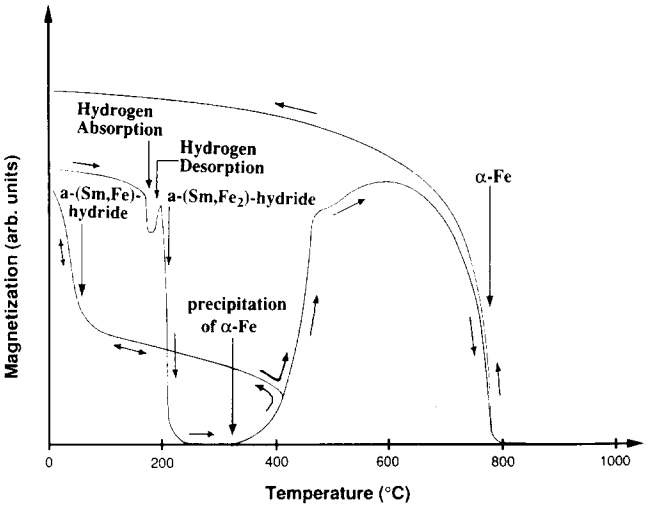

Fig. 10. TMA trace of an $SmFe_2$ sample sealed under an 'excess hydrogen gas" atmosphere with an initial ratio of $H/SmFe_2 = 4.8$.

phous phase together with Sm hydride. As the temperature increases, more α-Fe and Sm hydride precipitate resulting in a continuous change in the composition of the amorphous phase. On cooling from 410 °C, it was revealed (Fig. 8) that the T_c value of the amorphous phase (a-(Sm,Fe) hydride) was about 75 °C compared with 235 °C obtained for the amorphous phase (a-(Sm,Fe_2) hydride) shown in Fig. 7. Since the initial ratio of H atoms per mole of $SmFe_2$ was much greater than 2.6 (the maximum number of H atoms that one atom of Sm can absorb [26]), the final reaction products were α-Fe and Sm hydride as shown in the TMA trace on cooling from 840 °C (Fig. 10).

3.2.1.4. Hydrogenation reaction mechanism. Based on the experimental results obtained using the ITA, XRD and TMA, the following reaction mechanism is proposed for the "$SmFe_2 + H_2$" mixture placed in a heated constant volume reactor.

(i) Under a "deficient hydrogen gas" atmosphere

$$SmFe_2 + H_2(g) \longleftrightarrow SmFe_2 \text{ hydride} \quad (1)$$

$$SmFe_2 \text{ hydride} \longrightarrow \text{a-}(SmFe_2) \text{ hydride} \quad (2a)$$

$$SmFe_2 \text{ hydride} \longleftrightarrow SmFe_2 + H_2(g) \quad (2b)$$

$$\text{a-}(SmFe_2) \text{ hydride} \longrightarrow \text{a-}(Sm_{1-x}Fe_2) \text{ hydride} + x\text{Sm hydride} \quad (3)$$

$$\text{a-}(Sm_{1-x}Fe_2) \text{ hydride} \longrightarrow \text{a-}(Sm_{1-x_0}Fe_2) + \text{Sm hydride} \quad (4)$$

where x_0 is half of the initial ratio of H gas atoms per mole of $SmFe_2$ (assuming an Sm hydride of composition SmH_2)

$$\text{a-}(Sm_{1-x_0}Fe_2) \longrightarrow \alpha\text{-Fe} + \text{Sm} \quad (5)$$

Depending on the initial ratio of hydrogen gas atoms per mole of $SmFe_2$, one of the following reactions may occur (assuming that the Sm hydride composition is SmH_2)

$$\alpha\text{-Fe} + \text{Sm} + SmFe_2 \longrightarrow Sm_2Fe_{17} + \alpha\text{-Fe} \quad 1.53 < H/SmFe_2 < 2 \quad (6a)$$

$$\alpha\text{-Fe} + \text{Sm} + SmFe_2 \longrightarrow Sm_2Fe_{17} + SmFe_3 \quad 0.67 < H/SmFe_2 < 1.53 \quad (6b)$$

$$\alpha\text{-Fe} + \text{Sm} + SmFe_2 \longrightarrow SmFe_3 + SmFe_2 \quad 0 < H/SmFe_2 < 0.67 \quad (6c)$$

(ii) Under an "excess hydrogen gas" atmosphere

$$SmFe_2 + H_2(g) \longleftrightarrow SmFe_2 \text{ hydride} \quad (1)$$

$$SmFe_2 \text{ hydride} \longrightarrow \text{a-}(SmFe_2) \text{ hydride} \quad (2a)$$

$$SmFe_2 \text{ hydride} \longleftrightarrow SmFe_2 + H_2(g) \quad (2b)$$

$$\text{a-}(SmFe_2) \text{ hydride} \longrightarrow \text{a-}(Sm_{1-x}Fe_2) \text{ hydride} + x\text{Sm hydride} \quad (3)$$

$$\text{a-}(Sm_{1-x}Fe_2) \text{ hydride} + H_2(g) \longrightarrow \alpha\text{-Fe} + \text{Sm hydride} \quad (4)$$

The hydrogen absorption reaction seems to be initiated locally on the surface of the $SmFe_2$ sample. This observation was strongly suggested by the coexistence of $SmFe_2$ and $SmFe_2$ hydride phases. If the reaction were to take place homogeneously, no $SmFe_2$ phase should be observed but only $SmFe_2$ hydride. The exothermicity and local nature of the hydrogen absorption reaction are responsible for the development of local high temperature gradients which subsequently cause other reactions to occur (eqns. (2a), (2b) and (3)). This produces a mixture containing not only $SmFe_2$ and $SmFe_2$ hydride but also Sm hydrides and a-(Sm,Fe_2) hydride. The $SmFe_2$ hydride could be stabilized more easily under "deficient hydrogen gas" rather than "excess hydrogen gas" conditions (*cf.* Figs. 5(a) and 6(a)) because of the lower level of heat generated during hydrogen absorption.

Among the hydrides, the stability increases from the $SmFe_2$ hydride to the a-(Sm,Fe_2) hydride and finally to the Sm hydride. The hypothetical free energy diagrams proposed by Aoki *et al.* [4, 7] regarding the phase stability seem to be in accordance with the present results. However, it should be noted that the phase stability depends strongly on the details of the hydrogenation process such as the initial reaction conditions (H_2 pressure, $H/SmFe_2$ ratio and temperature) and the terminal hydrogenation temperature. For example, we can increase the presence of $SmFe_2$ hydride by heating

$SmFe_2$ at about 150 °C and then introducing small doses of hydrogen in such a way that excessive heats due to the hydrogen absorption reaction are minimized. On the other hand, we can suppress the hydrogen absorption reaction (1) by slowly charging the hydrogen at higher temperatures of about 300 °C. In this case the instantly formed $SmFe_2$ hydride is rapidly amorphized into a-($SmFe_2$) hydride and therefore its presence is diminished. If hydrogen is charged rapidly, an Sm-poor a-(Sm,Fe_2) hydride and Sm hydride will be formed instead.

3.2.2. Dehydrogenation

Amorphous $SmFe_2H_{3.2}$ (also containing a small amount of Sm hydride) was prepared inside the ITA under an initial ratio of $H/SmFe_2$ equal to 25 with heating up to 200 °C. Its ITA isochore trace was obtained under initial vacuum conditions as shown in Fig. 11. On heating, the solid rapidly begins to lose hydrogen between the temperatures of 160 and 200 °C. A more gradual loss of hydrogen was observed at higher temperatures. In the high temperature range (above 450 °C) and on cooling, only α-Fe and Sm hydride exist. This was confirmed by the XRD pattern obtained after cooling to room temperature. The final hydrogen composition ($SmH_{2.5}$) and the features of the ITA trace (on cooling) are consistent with the "$Sm+H_2$" system [26]. The loss of hydrogen from the amorphous phase is accompanied by the precipitation of Sm hydride. In this way, the amorphous phase constantly changes to Sm-poorer compositions. The XRD pattern obtained for a-($SmFe_2$) hydride after having been subjected to vacuum up to 200 °C showed that it was decomposed into Sm hydride and another Sm-poorer (Sm,Fe_2) hydride.

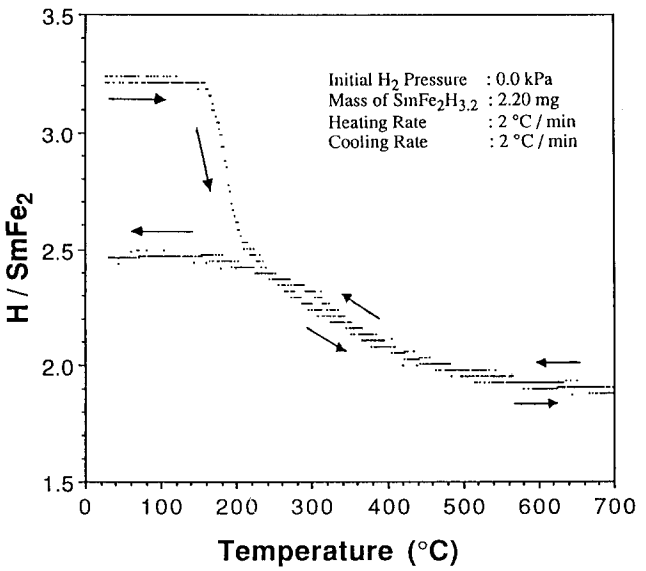

Fig. 11. ITA trace for a-$SmFe_2H_{3.2}$ under initial vacuum conditions.

3.3. Reaction of $SmFe_2$ with nitrogen

Figure 12(a) shows the ITA trace for the "$SmFe_2$(powder)$+N_2$" system. It suggests that the reaction is initiated at about 250 °C and is completed at high temperatures. The XRD patterns (Figs. 13(a)–13(c)) obtained for samples heated under the same conditions at 250, 450 and 950 °C show that, during the reaction (Figs. 13(a) and 13(b)), $SmFe_2$ coexists with α-Fe, Sm and SmN. No interstitial $SmFe_2$ nitride is found at any temperature. At 950 °C, the reaction is complete and only SmN and α-Fe exist (Fig. 13(c)). When a bulk $SmFe_2$ sample is used instead of powder, the reaction is initiated at about 450 °C but remains incomplete even after heating at 950 °C (Fig. 12(b)). The XRD pattern of this sample is shown in Fig. 13(d) and consists of SmN, α-Fe, Sm, $SmFe_2$ and some $SmFe_3$. It is obvious that the reaction is initiated at the surface of the $SmFe_2$ sample, where some of the Sm is tied up with nitrogen, and therefore the local metal composition (excluding Sm involved in SmN) is shifted to compositions between $SmFe_2$ and $SmFe_3$. This results in a local thermodynamic equilibrium between the $SmFe_2$ and $SmFe_3$ phases which are obtained after cooling to room temperature.

One possible reaction mechanism which can explain the coexistence of the four phases $SmFe_2$, α-Fe, Sm and SmN is that originally nitrogen causes the decomposition of $SmFe_2$ into α-Fe and Sm and subsequently it reacts with Sm to form SmN. This mechanism can also explain the slow reaction rate since it is controlled by the reaction between Sm and nitrogen, which is known [26] to be kinetically slow.

The nitrogenation reaction of $SmFe_2$ is very important for the Sm_2Fe_{17} nitride-based permanent magnets pro-

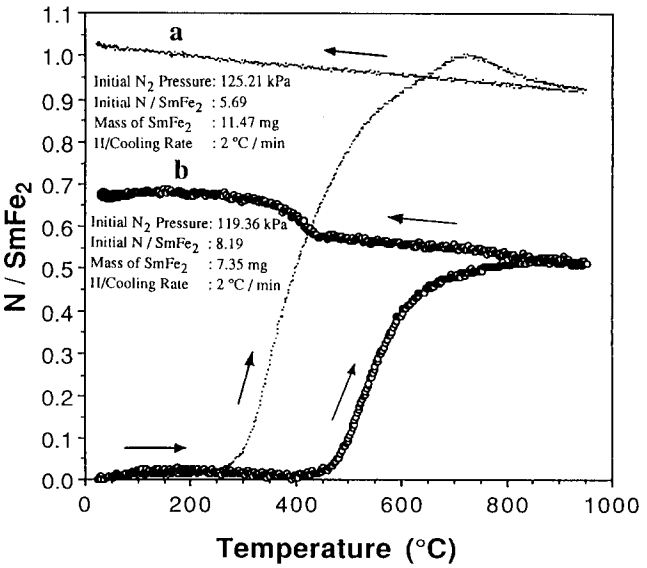

Fig. 12. ITA trace for the "$SmFe_2$(powder)$+N_2$" (a) and "$SmFe_2$(bulk)$+N_2$" (b) systems.

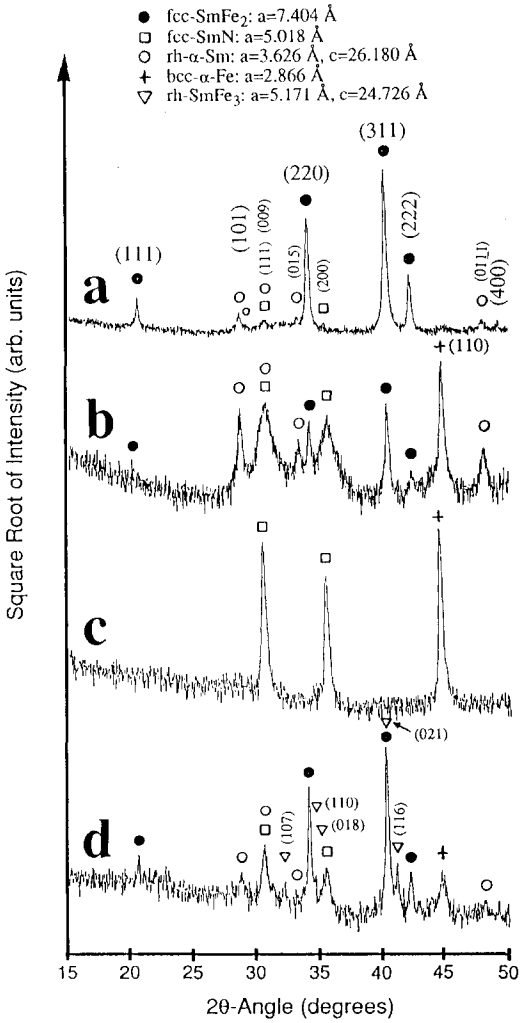

Fig. 13. XRD patterns. $SmFe_2$ powder nitrogenated at temperatures of (a) 250 °C, (b) 450 °C and (c) 950 °C. (d) Bulk $SmFe_2$ nitrogenated at 950 °C.

duced by rapid solidification [12, 13]. Before nitrogenation, the rapidly solidified Sm–Fe alloys consist mainly of the Sm_2Fe_{17} phase in metastable equilibrium with some $SmFe_2$ phase. During nitrogenation at about 450 °C, Sm_2Fe_{17} forms interstitial Sm_2Fe_{17} nitride which exhibits hard magnetic properties. On the other hand, $SmFe_2$ decomposes into the undesirable products α-Fe and SmN. Therefore the presence of the $SmFe_2$ phase in the rapidly solidified alloys is undesirable and should be eliminated.

4. Conclusions

The characteristics of the reaction between $SmFe_2$ and H_2 or N_2 have been studied by isochorothermal analysis, XRD and TMA and in terms of the reaction products obtained under different conditions (amount of gas and temperature). Possible hydrogenation products of $SmFe_2$ are $SmFe_2$ hydrides, a-(Sm,Fe_2) hydrides, Sm hydrides and α-Fe. If sufficient hydrogen is not available for reaction with all the $SmFe_2$, metastable elemental Sm and equilibrium phases such as $SmFe_3$ and Sm_2Fe_{17} are also produced. The Curie temperatures of the $SmFe_2$ hydride (110 K) and a-(Sm,Fe_2) hydride (75–235 °C) are far below that of the original $SmFe_2$ compound (410 °C). The hydrogenation mechanism of $SmFe_2$ involves the formation of $SmFe_2$ hydrides prior to the formation of a-($SmFe_2$) hydride. As the temperature increases, a portion of the a-(Sm,Fe_2) hydride crystallizes into Sm hydride resulting in an Sm-poorer a-(Sm,Fe_2) hydride. At about 325 °C, the amorphous phase begins to crystallize into both Sm hydride and α-Fe. In the absence of hydrogen, the terminal amorphous phase crystallizes into α-Fe and Sm.

Nitrogenation of the $SmFe_2$ phase causes the intermediate formation of α-Fe, Sm and SmN. No interstitial $SmFe_2$ nitride was found to exist at any temperature.

References

1 K. H. J. Buschow, *Physica B, 86–88* (1979) 79.
2 N. Kataoka, X-G. Li, K. Aoki and T. Masumoto, *J. Less-Common Met., 162* (1990) L11.
3 K. Aoki, K. Shirakawa and T. Masumoto, *Sci. Rep. Res. Inst. Tohoku Univ., Ser. A, 32* (1985) 239.
4 K. Aoki, T. Yamamoto, Y. Satoh, K. Fukamichi and T. Masumoto, *Acta Metall., 35* (1987) 2465.
5 P. Raj, P. Suryanarayama, A. Sathyamoorthy, K. Shashikala, K. V. Gopalakrishnan and R. M. Iyer, *J. Alloys Comp., 179* (1992) 99.
6 M. E. Kost, V. I. Mikheeva, M. V. Raevskaya, E. I. Yaropolova and A. L. Shilov, *Russ. J. Inorg. Chem., 24* (12) (1979) 1773.
7 K. Aoki, A. Yanagitani, T. Masumoto and K. Chattopadhyay, *J. Less-Common Met., 147* (1989) 105.
8 D. G. R. Jones, J. S. Abell and I. R. Harris, *J. Less-Common Met., 172–174* (1991) 1285.
9 J. M. D. Coey, H. Sun and Y. Otani, in S. G. Sankar (ed.), *Proc. Sixth Int. Symp. on Magnetic Anisotropy and Coercivity in Rare Earth–Transition Metal Alloys,* Pittsburgh, PA, October 25, 1990, p. 36.
10 K. Schnitzke, L. Schultz, J. Wecker and M. Katter, *Appl. Phys. Lett., 57* (1990) 2853.
11 M. Endoh, M. Iwata and M. Tokunaga, *J. Appl. Phys., 70* (1991) 6030.
12 C. N. Christodoulou and T. Takeshita, Sm_2Fe_{17}-nitride-based permanent magnets produced by rapid solidification, *J. Alloys Comp.,* in press.
13 M. Katter, J. Wecker and L. Schultz, *J. Appl. Phys., 70* (1991) 3188.
14 J. M. D. Coey and H. Sun, *J. Magn. Magn. Mater., 87* (1990) L251.
15 M. Q. Huang, L. Y. Zhang, B. M. Ma, Y. Zheng, J. M. Elbicki, W. E. Wallace and S. G. Sankar, *J. Appl. Phys., 70* (1991) 6027.
16 C. N. Christodoulou and T. Takeshita, Sm_2Fe_{17}-nitride-based permanent magnets prepared by HDDR, *J. Alloys Comp.,* in press.

17 H. Nakamura, K. Kurihara, T. Tatsuki, S. Sugimoto, M. Okada and M. Homma, *Digests of the 15th Annual Conference on Magnetics in Japan, October 29–November 1, 1991*, Magnetics Society, 1991, p. 379.
18 J. M. D. Coey, J. F. Lawler, H. Sun and J. E. M. Allan, *J. Appl. Phys., 69* (1991) 3007.
19 T. Mukai and T. Fujimoto, *J. Magn. Magn. Mater., 103* (1992) 165.
20 M. Q. Huang, B. M. Ma, W. E. Wallace and S. G. Sankar, in S. G. Sankar (ed.), *Proc. Sixth Int. Symp. on Magnetic Anisotropy and Coercivity in Rare Earth–Transition Metal Alloys, Pittsburgh, PA, October 25, 1990,* p. 204.
21 L. Y. Zhang, Y. Zheng and W. E. Wallace, in S. G. Sankar (ed.), *Proc. Sixth Int. Symp. on Magnetic Anisotropy and Coercivity in Rare Earth–Transition Metal Alloys, Pittsburgh, PA, October 25, 1990,* p. 219.
22 K. H. J. Buschow, R. Coehoorn, D. B. de Mooij, K. de Waard and T. H. Jacobs, *J. Magn. Magn. Mater., 92* (1990) L35.
23 J. M. D. Coey, H. Sun and D. P. F. Hurley, *J. Magn. Magn. Mater., 101* (1991) 310.
24 M. Q. Huang, Y. Zheng, K. Miller, J. M. Elbicki and S. G. Sankar, *J. Appl. Phys., 70* (1991) 6024.
25 D. P. F. Hurley and J. N. D. Coey, *J. Magn. Magn. Mater., 99* (1991) 229.
26 C. N. Christodoulou and T. Takeshita, *J. Alloys Comp.*, accepted for publication.
27 A. M. van Diepen, H. W. de Wijn and K. H. J. Buschow, *Phys. Rev. B, 8* (1973) 1125.
28 K. Aoki, M. Nagano, A. Yanagitani and T. Masumoto, *J. Appl. Phys., 62* (1987) 3314.